Available online at www.sciencedirect.com

ScienceDirect

Ciência & Tecnologia dos MATERIAIS

http://ees.elsevier.com/ctmat

Ciência & Tecnologia dos Materiais 29 (2017) e9–e14

Special Issue "Materiais 2015"

Correlation between the Meyer's law parameters and the wear resistance of chromium white cast irons

L. Goyos[a, *], A. Varela[b], S. Castellanos[a], A. García[b], J. Mier[b], M. Moors[c]

[a]*Dept. Ciencias de Energía y Mecánica, Universidad de las Fuerzas Armadas ESPE, Ave. General Rumiñahui s/n, Valle de los Chillos, Ecuador. CP 15701*

[b]*Grupo de Investigación en Ciencia e Ingeniería de Materiales, Universidade da Coruña, Mendizábal s/n, Ferrol, CP 15403, España*

[c]*Toegepaste Materiaalwetenschappen, Gent Universitiet, Technologiepark 903, 9052 Zwijnaarde, Gent, België*

Abstract

This work studies plastic behaviour and its influence on the abrasive wear resistance of a group of high chromium white cast irons. The irons were poured in metallic moulds and heat treated. The studied alloys have 3% C, 12% Cr, as well as 0.6% and 2.4% Si. The plastic characteristics are evaluated through the parameters obtained from Meyer's test: the strain hardening capacity (n) and the constant of penetration resistance (k).

The influence of silicon content and applied heat treatments on Meyer's test parameters was determined. The heat treated samples showed values between n=2.3 and n=2.5. These values confirm a hardening capacity greater than the cast specimens. The high silicon alloy specimens show greater n-values than the low silicon alloy ones. This tendency is remarked when the complete treatments (austenitizing, cooling and holding) are applied. Correlation between n, k and the relative abrasive wear show good values for (k), but too much dispersion for the Meyer's Index (n).

Keywords: White cast iron; heat treatment; abrasive wear; strain hardening; Meyer's test.

1. Introduction

The high abrasive wear resistance and relatively good impact resistance of high chromium white cast irons (HCCI) have facilitated their frequent use for the mining and quarry industry [1-5]. The characteristics and properties of these irons have been studied, so much regarding the matrix structure [6-10], the size and orientation of the primary carbides [11,12], or their heat treatment and subsequent precipitation of secondary carbides [8,10,13-16].

Heat treatments are widely used in these foundries and alloying elements guarantee the hardenability for thick parts. Molybdenum has been the favourite addition element, also combined with nickel and copper, among others [17-19]. The use of silicon additions in these irons has been limited and it associates with low wear resistance due to the presence of perlite [5,20]. Nevertheless, silicon regulates the precipitation of carbides and the proportions in the matrix of the different phases [17,21]. Santofimia [21] pointed out the silicon content influence on the bainitic transformation and the residual austenite. Tripathy and Pattyn [18,22,23] reported the bainitic transformation as a factor for the wear resistance improvement.

Typically the hardening heat treatment of high chromium cast irons performs an austenitizing to destabilize the austenite and guarantee the desired hardenability [14,20,24]. The sub-critical treatment, done below the transformation temperature and without previous austenitizing, is attractive due to its relative low costs and good results [5,8,25].

* Corresponding author.

E-mail address: llgoyos@espe.edu.ec (L. Goyos)

http://dx.doi.org/10.1016/j.ctmat.2017.05.002

As reported by Dodd, Maratray and other authors [8,26-28] the solidification speed must be selected in relation with the chemical composition to obtain an appropriate microstructure. Bedolla and Rainforth [28] have reported a refinement of the structure and a secondary carbides volume increase in the 17Cr-Ni-Mo alloy, with variables amounts of Si, poured in metallic moulds. They also reported a maximum wear resistance for silicon content to be around 2%.

The strain hardening plays an important role for wear resistant applications because they are typically involved in operations with high surface loads. The addition of manganese and other alloying elements has been used to increase the austenite presence and therefore the strain hardening capacity [1,29-31], and to improve the balance between the abrasive wear resistance and the impact resistance. It is reported also that the ferrite can play a role in complex microstructures [31-33]. There are practically no references regarding the wear behaviour and strain hardening ability of other structures, particularly the ferrite or complex structures in the HCCI.

Zum Gahr [12,34], regarding the influence of the microstructure on abrasive wear, proposed a model for the two bodies abrasion. This model shows the influence on wear from the strain hardening ability of the material related to its plastic behaviour. It is demonstrated that, in spite of the similarity between the penetration test and the cutting action of the abrasive particle, the attempts of correlating the hardness with the abrasive wear have been successful only in a very general way. According to this author [35], it happens because the strain hardening has different effects on wear resistance and hardness, and also because the interactions abrasive-material are not completely characterized. Working on different matrixes, this author highlights the different situations that can be presented and concludes that the ratio of the hardness measured after and before the deformation, which is the magnitude of the strain hardening, shows a different influence on abrasive wear resistance in function of the ductility of the analysed microstructural phase. This situation remarks the importance of studying the plastic behaviour of abraded materials.

Most of the reported studies quantify the strain hardening by means of hardness measurements along a direction perpendicular to the working surface. This method evaluates the effective deformation but it is not an intrinsic property of the material, as the strain hardening capacity.

Although the strain hardening coefficient is determined performing the tensile test, it is known [36-38] that the Meyer´s Index can give an indirect evaluation of the strain hardening ability of a given material. The law of Meyer relates the loads applied with the diameter of the indentations obtained in a hardness test [37]:

$$P = k\, d^n \quad (1)$$

The value of the exponent in Eq. (1) is known as the Meyer´s Index and its values vary between 2 and 2.5, being smaller as minor is the strain hardening ability. The fractional part of the Meyer´s Index coincides with enough accuracy with the value of the strain hardening coefficient obtained from the stress-strain curve. The logarithmic expression of Eq. (1) is:

$$\ln P = \ln k + n \ln d \quad (2)$$

The value of n is determined as the slope of the regression line of the logarithmic plot. Also from the plot it is possible to evaluate the penetration resistance (k), without the influence of the strain hardening ability of the material. The line intersection on the axis of loads represents the necessary load to obtain a unitary indentation and is not affected by the strain hardening process.

This work focuses the influence of composition and heat treatment of high chromium cast irons on the Meyer´s Index (n) and the penetration resistance (k) as estimators of the plastic behaviour of these alloys. The relation between these estimators and the abrasive wear is also studied to evaluate the potential influence of the plastic behaviour on the abrasive wear resistance.

2. Materials and Methods

The studied alloys have the composition shown in Table 1. Synthetic pig-iron, ferro-chromium primary alloy and low carbon ferrosilicon were used for the melting process. A 5 kg capacity high-frequency induction furnace was used. The alloys were poured in metallic strip ingot moulds (see Fig. 1) at 1380ºC. Because the strip ingot moulds are open in the top, the heat flows mainly through the bottom of the mould and the main direction of the dendrites growth is perpendicular to the bottom surface of the mould and the strips obtained. The dimensions of the strips obtained were 15x8 mm and 250 mm long. Specimens with dimensions 15x15 mm were cut along the strip.

Fig. 1. Metallic strip ingot mould used.

So, the surface of the specimen used for the abrasion and Meyer´s tests is obtained from the bottom surface of the strip. It guarantees that the testing surface of each element is perpendicular to the main heat evacuation direction and the axis of the primary dendrites. A total uniformity is assured for the characteristics of the testing surfaces, although this orientation is the less favourable for the resistance to abrasive wear. By machining, the final dimensions of the specimens were 15x15x5 mm.

Table 1. Chemical composition of the alloys.

Alloy	C (%)	Cr (%)	Si (%)	Mn (%)
High Si (A)	3.02	12.02	2.4	0.51
Low Si (B)	3.05	12.10	0.63	0.5

Alloys were heat treated as shown in Table 2, where it is used the alloy designation “A” for the high silicon alloy as-cast, “B” for the low silicon alloy as-cast and “AT” and “BT” for the heat treated alloys. Two different heat treatments were applied. The first one consisted in austenitizing treatment at 970ºC for one hour, followed by air cooling to 250ºC and then maintained at this temperature during 45, 90, 180 and 360 min. In Table 2 these heat treatments are designated as Au + H[XX] where the values in brackets are the holding time in minutes. The second treatment was an isothermal holding in the heat treatment furnace at 250ºC, directly from the as-cast state, during 180 and 360 min. In these-heat treatments the designation in Table 2 is H[XX] where XX is the holding time in minutes. Temperatures and times were selected pursuing to work in the bainitic region, based on works of Maratray and Pattyn [14,18].

Abrasive wear tests were performed using a pin-on-disc tribometer. The pin was substituted by the specimen tested and its biggest surface was placed against the disc. A force of 30 N was applied, using corundum grain 80, along a distance of 500 m. The magnitude of the worn out layer was evaluated by measuring the reduction of the diagonal of the pyramidal indentations carried out in the extreme points and in the centre of the sample. Three specimens of each sample were evaluated, using the average of the results.

The determination of the Meyer’s Index (n) and the Penetration Resistance (k) were performed using a 5 mm diameter tungsten carbide spherical indenter. Loads of 4291 N, 9194 N, 14097 N and 19000 N were applied. The obtained indentations did not go beyond half of the diameter of the indenter. The indentations were applied in two test specimens of each sample and were measured with a 20x ocular and minimum appreciation of 0.005 mm.

Table 2. Designation, heat treatment and some properties of samples studied.

Alloy designation	Heat treatment	Hardness (HRC)	Austenite content (%)	Meyer´s Index value	Penetration Resistance (N)
A	As-cast	55	0	2.05	4339
B	As-cast	55	0	2.09	3843
AT45	Au + H[45]	52	0	2.43	3593
BT45	Au + H[45]	53	0	2.41	2829
AT90	Au + H[90]	52	0	2.48	3303
BT90	Au + H[90]	53	6.7	2.42	3399
AT180	Au + H[180]	52	4	2.45	2267
BT180	Au + H[180]	51	10	2.40	2304
AT360	Au + H[360]	52	0	2.50	2600
BT360	Au + H[360]	52	7.3	2.34	3255
A180	H[180]	55	0	2.30	3719
B180	H[180]	56	0	2.28	3718
A360	H[360]	55	0	2.36	3812
B360	H[360]	56	0	2.32	4132

Note: All austenitizing treatments (Au) were performed at 970ºC during 1 hour. All holding treatments (H) were performed at 250ºC during the time (in minutes) shown in brackets.

Each measurement was repeated 5 times and the average of the lectures for both test specimens was used. The regression line of the applied loads versus indentation diameters was determined in a log-log plot. The coefficients of regression of these adjustments (r^2) were in most cases greater than 0.99 and deviations did not exceed the value of 4.10^{-4}.

The metallographic observation was carried out by means of optical and scanning electron microscopy. The presence of the alloying elements in matrix and carbides was determined by energy dispersive spectrometry and the austenite content using X-ray diffractometry (radiation MoK, 30 kV, 25 mA) according to ASTM St E975-84. For the carbide volume quantification the method proposed by Maratray [14] was implemented, using the digital images of the samples.

3. Results and Discussion

Both alloys present small carbides distributed in the typical dendritic pattern of hypoeutectic alloys. The high silicon alloy evidence smaller, more rounded and more disperse carbides than the low silicon alloy, as can be appreciated in Fig. 2. The volume of primary carbides of the high silicon alloys reaches a value of 16.8 ± 1.7% while the low silicon alloy has 18.6 ± 2.4%.

These values are approximately 5% lower than expected for the same alloys but sand cast, according to formula proposed by Maratray [14].

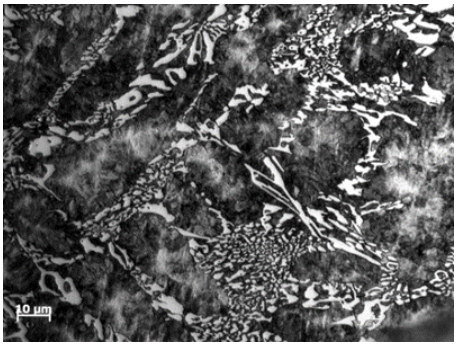

a)

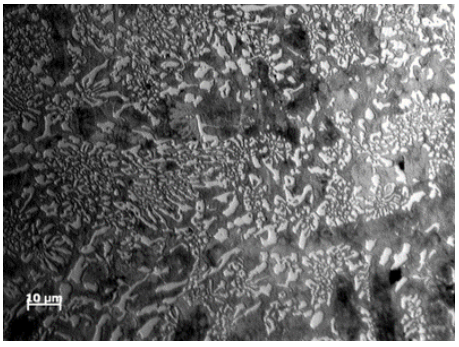

b)

Fig. 2. Microstructure of the alloy with low silicon (a) and high silicon (b), as-cast.

Both alloys as-cast show a matrix of fine perlite. There is no evidence of austenite, martensite or intermediate products in the as-cast samples. The hardness of both alloys is high and practically the same, as shown in Table 2.

The applied treatment of austenitizing and ulterior holding at 250ºC for different times had no apparent influence in the matrix structure of any of the alloys. The different heat treatments have led to a very fine perlitic structure without preferable orientation.

Only small volumes of austenite are present, always in austenitized samples and mostly for low silicon alloy (see Table 2). The maximum of austenite content is presented in the Au + H treatment for 180 min holding. Secondary carbides are present in the specimens heat treated with austenitizing and ulterior holding. This heat treatment propitiates the combination of carbide forming alloying elements retained in the structure during the high speed solidification. Slightly bigger quantities of the secondary carbides are present in the high silicon alloy, as observed in Fig. 3.

There is no secondary carbides precipitation in the sub-critical treatments. In these samples the fine perlitic structure remains. There is no austenite presence, according to diffractometer analysis.

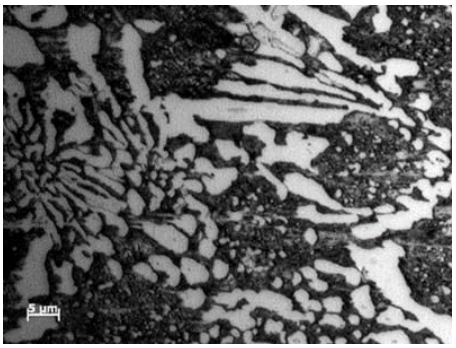

a)

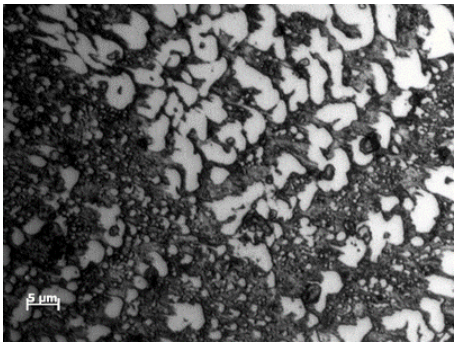

b)

Fig. 3. Microstructure of the alloy with low silicon (a) and high silicon (b), after heat treatment Au + H[360].

The behaviour of the Meyer´s Index “n” and the penetration resistance “k” is shown in Fig. 4. The as-cast samples present n-values near 2, which implies a minimum strain hardening capacity as a consequence of the residual stresses generated by the high solidification rate. The heat treated samples present n-values over 2.25. This value evidences a hardening capacity greater than the as-cast samples. The high silicon samples present n-values commonly bigger than the low silicon samples, regardless the heat treatment applied. This behaviour is caused by the relaxation of the stresses and the transformation of the structure toward more plastic components.

On the other hand, the austenitizing and holding treatment propitiates the precipitation as secondary carbides of the carbon retained in the lattice by the silicon action. This carbon depletion of the lattice increases the ductility of the matrix and creates a precipitate which constrains the dislocation displacements, increasing the strain hardening effect. The sub-critically treated samples, which do not present secondary carbide precipitation, have n-values lower than the austenitized samples which reinforces the explanation.

It is remarkable that the austenitized samples with high austenite volume do not have the greatest n-values. The behaviour of the low silicon samples is practically the same for holding times till 180 min and decreases for the 360 min holding.

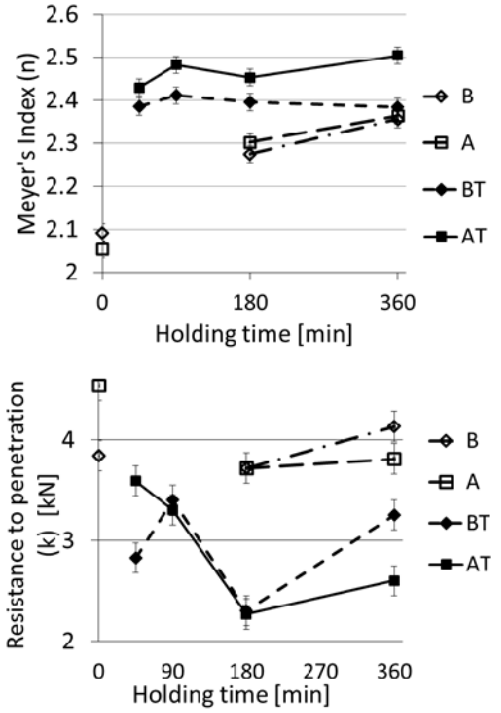

Fig. 4. Evolution of "n" values and "k" values in relation to heat treatment and silicon content.

The behaviour is totally different for the high silicon samples, with a clear increase of the n-values for 360 min holding. This behaviour suggests that the austenite content is not the main factor in the strain hardening ability evolution of these alloys, under the deformation conditions applied.

The k-values follow a tendency somewhat opposite to n-values. The high silicon samples have lower k-values than the low silicon ones. This behaviour is marked for the 360 min holding treatment. This holding time is the closest to bainitic transformation region for the high silicon alloy. For this holding time, it is expected the greatest formation of the ferrite-carbide conglomerate during solidification and the maximum of secondary carbides precipitation during the heat treatment. In a similar way, the k-values corresponding to as-cast and sub-critically treated samples are greater than the k-values of samples with austenitizing and holding treatment. The minimum k-values coincides with the maximum austenite content for high silicon alloy as well as for the low silicon content. This behaviour denotes a greater Resistance to Penetration in the samples less relaxed by the heat treatment, and a lower resistance in those with softer structures. The relative wear behaviour of samples with different treatments applied is shown in Fig. 5, ordered according to the k-values and n-values.

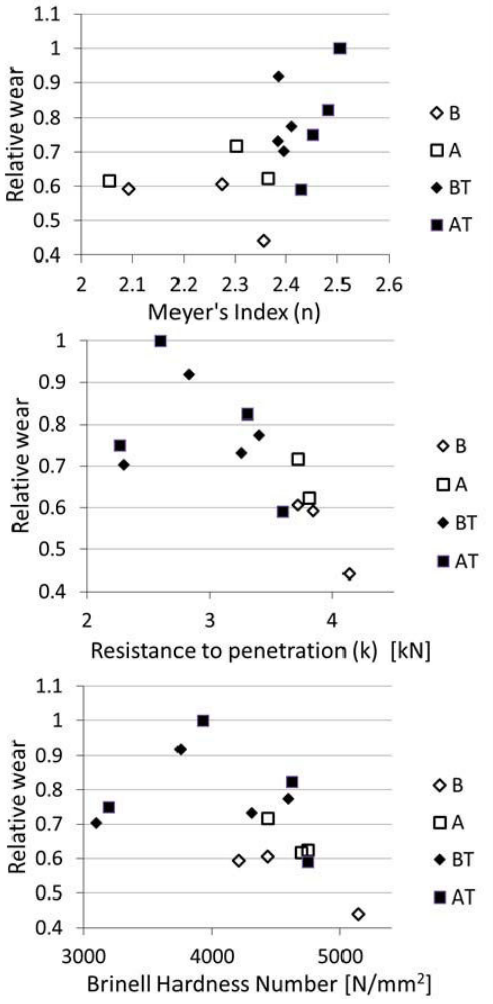

Fig. 5. Influence of Resistance to Penetration, Meyer's Index and Hardness on relative wear.

The relative wear shows an appreciable tendency to decrease when the k-value increases, i.e., as the Resistance to Penetration increases. This trend is valid for the high and low silicon alloys, as well as for the different heat treatment applied. Only the as-cast samples differ from this trend, which are the hardest and have a stressed structure. This is a completely different condition from the rest of the samples. It is important to point out that this trend remarks the significance on the wear resistance of the Resistance to Penetration (k) obtained from Meyer´s test.

By comparing the graphs in Fig. 5, it is noticed that the correlation between the relative wear and the k-values is narrower than the correlation between the

hardness values and the relative wear. It suggests that the Resistance to Penetration (k) could be a better indicator of the wear resistance than the conventional hardness, which is affected by the strain hardening effect.

The correlation between relative wear and n-values shows a different behaviour. The as-cast samples again differ from the general behaviour because of their stressed structure and, therefore, show n-values closer to the lower end of the interval. As it can be noticed, a clear tendency is not present in the graph. Moreover, analysing the groups of samples separately it is evident that there are no common patterns. The n-values are grouped in two narrow bands, corresponding to high and low silicon alloys.

4. Conclusions

The fast solidification conditions of high chromium cast irons produces a very hard casting structure which has very low plasticity and strain hardening ability. The addition of silicon to the studied alloy increased the strain hardening capacity.

The application of heat treatment causes a relaxation of the structure and boosts the strain hardening capacity. This property reached its highest values in the studied samples with austenitizing and holding treatment.

It is possible to correlate the abrasive wear resistance of these alloys with the Resistance to Penetration (k) obtained from the Meyer's test. The abrasive wear decreases as the Resistance to Penetration (k) increases in the heat treated samples.

There was no correlation found between the abrasive wear and the strain hardening capacity (n), obtained from the Meyer's test.

Acknowledgements

The authors acknowledge the scholarship granted by Programa Prometeo, SENESCYT, Ecuador, to L.G.P.

References

[1] H.S. Avery, Work hardening in relation to abrasion resistance, Proceedings of the Symposium on Materials for the Mining Industry, Vail, Colorado, USA, July 30-31, 1974, Climax Molybdenum Co., p. 43.
[2] J. Dodd, J.L. Parks, Factors affecting the production and performance of thick section high-chromium-molybdenum alloy iron casting, Climax Molybdenum (Ed.), Climax Molybdenum, Greenwich, Connecticut, USA, 1980, M383E-15M.
[3] G. Laird, AFS Trans. 101 (1993) 97.
[4] F. Maratray, Bull. Cercle Etud. Met. (1979) 11.
[5] J.L. Parks, Reprint Transactions AFS 1978, Climax Molybdenum (Ed.), Climax Molybdenum, Vail, Colorado, USA, 1978, M-358.
[6] J. Asensio, J.A. Pero-Sanz, J.I. Verdeja, Mater. Charact. 49(2) (2003) 83.
[7] O.N. Dogan, J.A. Hawk, AFS Trans. 105 (1997) 167.
[8] L. Goyos *et al.*, Rev. Metal. 48(4) (2012) 277.
[9] R.B. Gundlach, AFS Trans. 82 (1974) 309.
[10] K.K. Singh, R.S. Verma, G.M.D. Murty, J. Mater. Eng. Perform. 18 (2009) 438.
[11] O.N. Dogan, J.A. Hawk, Wear 189 (1995) 136.
[12] K.H.Z. Gahr, G.T. Eldis, Wear 64 (1980) 175.
[13] A. Bedolla-Jacuinde, L. Arias, B. Hernández, J. Mater. Eng. Perform. 12(4) (2003) 371.
[14] F. Maratray, R. Usseglio-Nanot, Atlas Transformation characteristics of Cr and Cr-Mo white irons, Climax Molybdenum, Belgium, 1970, p. 198.
[15] Z. Sun *et al.*, Mater. Charact. 53 (2004) 403.
[16] G. Berg, P. Grau, Cryst. Res. Technol. 32(1) (1997) 149.
[17] C. Cetinkaya, Mater. Des. 27 (2006) 437.
[18] R.L. Pattyn, AFS Trans. 102 (1994) 107.
[19] L. Wei, J. Iron Steel Res. Int. 14(3) (2007) 47.
[20] W.W. Cias, AFS Trans. 82 (1974) 317.
[21] M.J. Santofimia, PhD thesis, Universidad Complutense de Madrid, Spain, 2006.
[22] R.L. Pattyn, AFS Trans. 101 (1993) 161.
[23] I. Tripathy, MSc thesis, National Institute of Technology Rourkela, India, 2011.
[24] J. Wang *et al.*, Mater. Charact. 55 (2005) 234.
[25] I. Fernández-Pariente, F.J. Belzunce-Varela, Rev. Metal. 42(4) (2006) 279.
[26] J.J. Coronado, A. Sinatora, Wear 267 (2009) 2116.
[27] F. Maratray, R. Usseglio-Nanot (Ed.) Factors affecting the structure of chromium and chromium-molybdenum white irons. Climax Molybdenum S.A., Paris, France, 1970, p. 32.
[28] A. Bedolla-Jacuinde, W.M. Rainforth, Wear 250 (2001) 449.
[29] B.A. Bertoli, Rev. Latinoam. Sider. (1975).
[30] H. Martínez, L. Goyos, Rev. C. Maq. 13(4) (1988).
[31] R.S. Jackson, Proceedings of Colloque International sur les alliages ferreux à hautes teneurs en chrome et en carbone, Cercle d'études des métaux, Saint-Etienne, France, 1973.
[32] C. Diez, L. Goyos, U. Ordoñez, El índice de endurecimiento en las fundiciones nodulares austemperadas, Proceedings of III Congreso Iberoamericano de Ingeniería Mecánica, La Habana, Cuba, September, 1997.
[33] V. Abouei, H. Saghafian, S. Kheirandish, Wear 262, (2007) 1225.
[34] K.H.Z. Gahr, Wear 124 (1988) 87.
[35] K.H.Z. Gahr, Tribol. Int. 31(10) (1998) 587.
[36] G. Dieter, Mechanical Metallurgy, 3rd ed., McGraw-Hill, 1988, p. 766.
[37] D. Tabor, The Hardness of Metals, Oxford University Press, New York, 1951.
[38] S. Riveros, Aceros antiabrasivos. Medición del índice de endurecimiento Meyer y predicción del edurecimiento adicional en uso según técnica de Tabor, Proceedings of CONAMET/SAM, La Serena, Chile, November 3-4, 2004.